

Properties Study of ZnS Thin Films Prepared by Spray Pyrolysis Method

A. Djelloul^{1,2,*}, M. Adnane¹, Y. Larbah¹, T. Sahraoui¹, C. Zegadi¹, A. Maha², B. Rahal³

¹ Laboratory of Electron Microscopy and Materials Sciences University of Science and Technology of Oran, B.P. 1505, 31000 El-Mnaouer Oran, Algeria

² Centre de Recherche en Technologie des Semi-Conducteurs pour l'Energétique 'CRTSE' 02 Bd Frantz Fanon. B.P. 140, 7 Merveilles, Alger, Algérie

³ Nuclear Research Center of Algiers (CRNA), 2 Bd., Frantz Fanon, BP 399, Algiers 16000, Algeria

(Received 07 October 2015; published online 10 December 2015)

Zinc sulfide (ZnS) is important II-VI semiconductors material for the development of various modern technologies and photovoltaic applications. ZnS thin film was prepared by using chemical spray pyrolysis technique. The starting solution is a mixture of 0.1 M zinc chloride as source of Zn and 0.05 M thiourea as source of S. The glass substrate temperature was varied in the range of 300 °C-400 °C to investigate the influence of substrate temperature on the structure, chemical composition, morphological and optical properties of ZnS films. The DRX analyses indicated that ZnS films have polycrystalline cubic structure with (111) preferential orientation and grain size varied from 25 to 60 nm, increasing with substrate temperature. The optical properties of these films have been studied in the wavelength range 300-2500 nm using UV-VIS spectro-photometer. The ZnS films has a band gap of 3.89 eV-3.96 eV.

Keywords: ZnS, Spray Pyrolysis, DRX, UV-VIS, Band gap.

PACS numbers: 81.05.Dz, 78.66.Hf, 61.05.Cp,
78.66. – Hf

1. INTRODUCTION

Zinc sulphide belongs to II-VI group compound material with large direct band gap < 3.50 eV depending upon composition. Zinc sulphide (ZnS) is an important semiconducting material with a wide direct band gap and *n*-type conductivity is promising for optoelectronic device applications, such as electroluminescent devices and photovoltaic cells [1-4]. Several techniques on growing ZnS thin films have been reported, which include Spray Pyrolysis (SP) [5, 6], Successive Ionic Layer Adsorption and Reaction (SILAR) [7-10], RF sputtering [11], Chemical Bath Deposition (CBD) [12-18], Molecular Beam Epitaxy (MBE) [19], Dip Technique (DT), Pulsed-Laser Deposition (PLD) [20], Chemical Vapour Deposition (CVD) [21].

In present investigation ZnS thin films have been deposited using Chemical Spray Pyrolysis techniques. The morphological, structural and optical properties of the as deposited ZnS thin films were studied.

2. EXPERIMENTAL DETAILS

2.1 Materials and Methods

Thin films of ZnS are prepared by Spray Pyrolysis technique. Spray Pyrolysis is basically a Chemical deposition technique in which fine droplets of the desired material solution was sprayed onto a heated substrate. The experimental Setup used for the preparation of pyrolytically spray deposited films is described here. The initial solution was prepared with one part of 0.1 M ZnCl₂ and one part 0.1 M SC(NH₂)₂ [thiourea] in deionized water. The deposition temperature was 300 °C-400 °C, the distance between the substrate and the spray gun nozzle was fixed at 35 cm. A schematic

drawn of the spray pyrolysis apparatus for the synthesis of the ZnS particles is depicted in Figure 1. The morphological, optical, structural and compositional analysis of films has been investigated by SEM, UV spectroscopy; XRD and EDAX.

3. CHARACTERIZATIONS

The surface morphologies of films were examined by electronic microscopy (SEM) (JEOL, (JSM-6610LA)). The structural characterization of the films was analyzed using X-ray diffractometer (XRD) (Siemens D500) with Cu K α radiation. The Fourier Transform Infrared (FTIR) spectra of the samples were recorded using JASCO FI-IR 460 spectrometer by KBr pellet technique in the range 400-4000 cm⁻¹. The resistivity of the samples

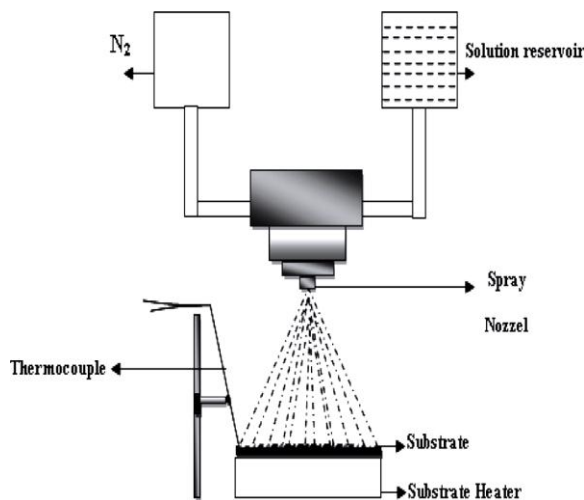


Fig. 1 – Schematic diagram of spray pyrolysis process of ZnS preparation

* djelloulertse@gmail.com

and the gas sensing was measured using a two-point probe conventional instrument. The optical transmittance measurements of the films were performed with a UV-Visible spectrophotometer (Cary 500).

4. RESULTS AND DISCUSSION

4.1 Morphological Properties

The scanning electron microscopy technique is familiar for the study of surface morphology of metal chalcogenides in the thin film form. The ZnS film prepared with optimized parameters is used for SEM observation. SEM images of ZnS thin films deposited on glass substrate at different substrate temperatures ($T_s = 300\text{-}400\text{ }^\circ\text{C}$) are shown in Fig. 2 (a, b and c).

The surface of the thin films displays an inhomogeneous appearance in all scanned areas of the sample as shown in Fig. 2.

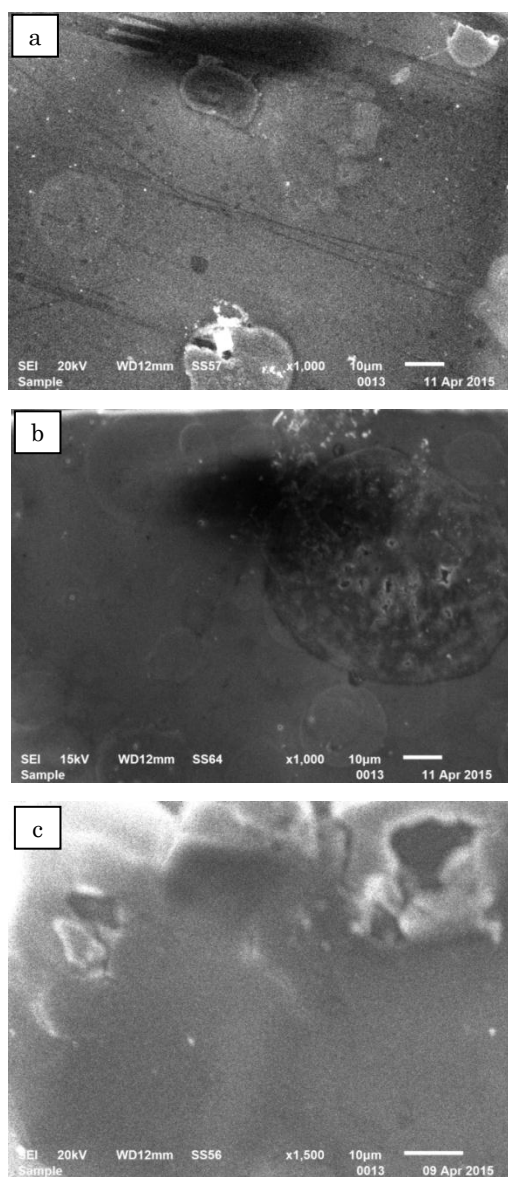


Fig. 2 – Scanning Electron microscopy as deposited ZnS on glass substrate at: 300 °C sprayed (a), 350 °C sprayed (b) and 400 °C sprayed (c)

4.2 Structural Properties

The X-ray diffraction pattern of ZnS films is also reported in the present work with the help of a Philip X-ray diffractometer by using CuK α radiation ($\alpha = 1.54045\text{ \AA}$).

The average grain size was calculated from the Scherrer formula, which involve the width of the X-ray diffraction line [22].

$$D = \frac{K\lambda}{\beta \cos \theta} \quad (1)$$

Where:

D is the mean particle size.

β is the full width at half maximum (FWHM in radians) of the peak corrected for instrumental broadening, and θ is the diffraction / Bragg's angle.

λ is the wavelength of the X-ray radiation (0.15406 nm). K : is the Scherer constant, it is value is taken as 0.9 for the calculations [23-25].

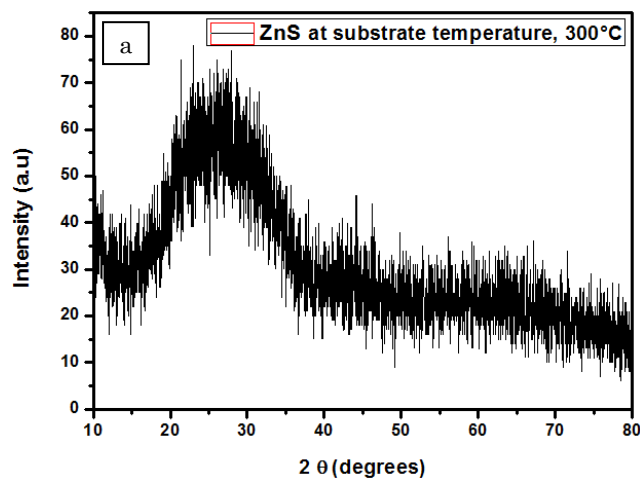
The grain size of ZnS thin films were found to be about 25 nm and 60 nm.

X-ray diffraction profiles of ZnS thin films prepared at various substrate temperatures ($T_s = 300\text{-}400\text{ }^\circ\text{C}$) are shown in Fig. 3 (a, b and c). One can note the progressive emergence of the diffraction peak located at 28° underlining a strong preferential orientation growth perpendicular to the crystallographic plans (111), which corresponds to ZnS cubic structure [26]. The intensity of the peak is enhanced with increasing the substrate temperature; it becomes intense when the substrate temperature is equal to $400\text{ }^\circ\text{C}$.

In Fig. 4, a typical EDX spectrum for ZnS film is indicated. The films used in this analysis are deposited at substrate temperature, $400\text{ }^\circ\text{C}$. As can be seen, films are composed of S and Zn.

According to XRD diffraction results (Fig. 3 (a) and (b)), films deposited at low temperature have an amorphous structure, since no peaks is present in the XRD diffraction pattern, or at least it is composed with a small crystallite size.

The Fourier transform infrared (FTIR) measurements were undertaken to confirm the formation of the thin films. Fig. 5 (a) and (b) shows the FTIR spectra of



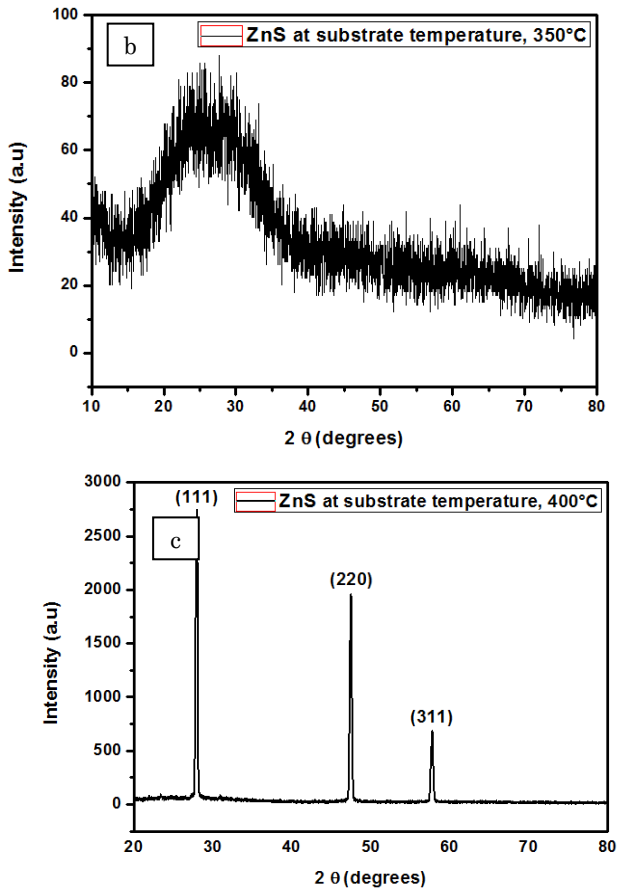


Fig. 3 – X-ray diffraction pattern of sprayed ZnS film at substrate temperature: 350 °C (a), 350 °C (b) and 400 °C (c)

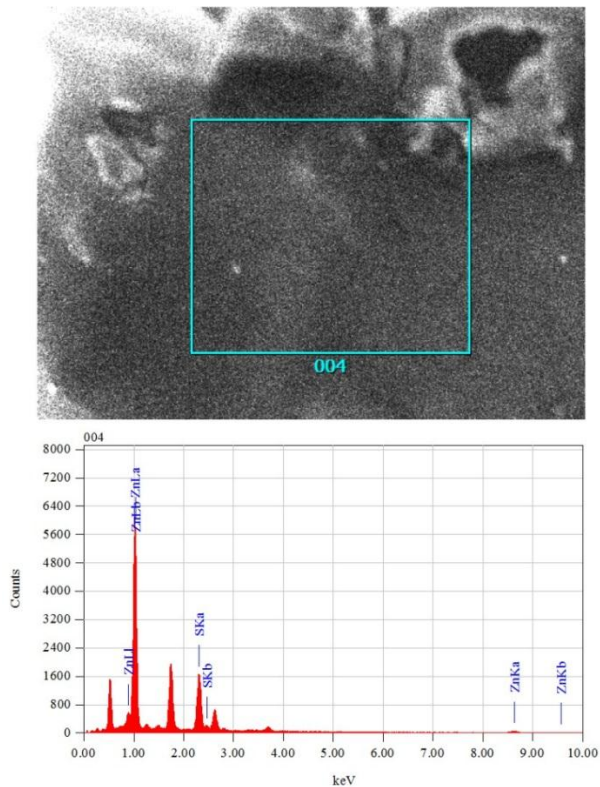


Fig. 4 – SEM micrograph spectrum analysis and EDAX of ZnS thin film at substrate temperature, 400 °C

ZnS thin film at substrate temperature, 350 °C and at 400 °C respectively. It can be seen that each sample shows a weak characteristic vibrations of zinc sulfide located at 611.45 and 680 cm^{-1} , others peaks are attributed to the formation of ZnS nanoparticles.

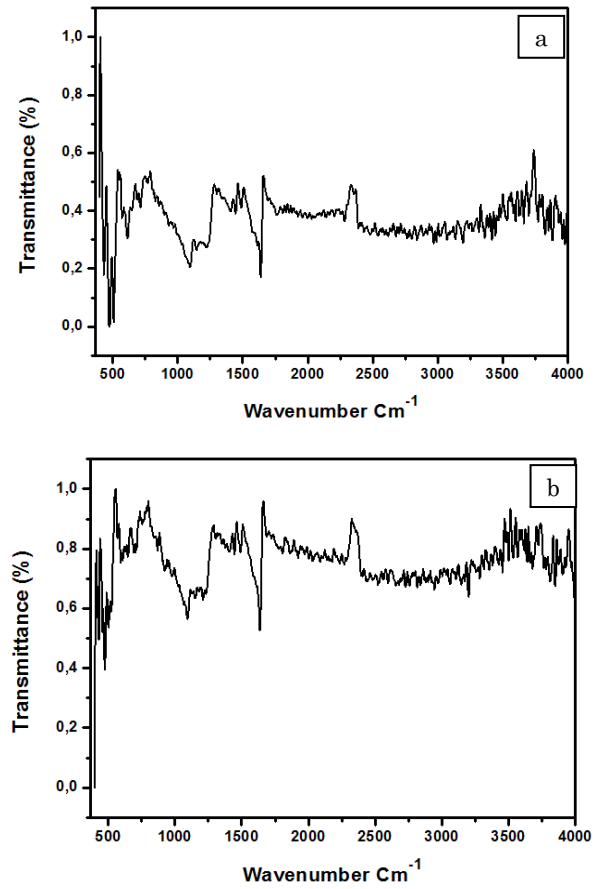


Fig. 5 – FTIR Spectrum of ZnS thin film at substrate temperature, 350 °C (a) and 400 °C (b)

4.3 Optical Properties

Optical transmission and reflection for the ZnS thin films on glass substrates were measured in the range (300-2500 nm) using a spectrophotometer. The spectral transmittance curves of these films are shown in Fig. 6.

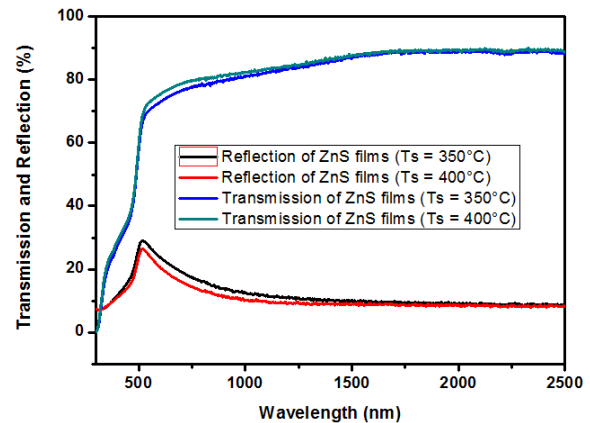


Fig. 6 – Optical transmission and reflection spectra of ZnS thin films prepared at various substrate temperatures ($T_s = 350$ °C and 400 °C)

Fig. 6 shows the transmittance of ZnS films prepared at various substrate temperatures ($T_s = 350\text{ }^\circ\text{C}$ and $400\text{ }^\circ\text{C}$). As can be seen, an increase in the substrate temperature improves the films optical transmission. It passes from 50 % to 90 % at the incident wavelength of 600 nm. Generally, the film transmittance is increased with the reduction of film thickness.

However, in our case, the transmittance improvement cannot be explained in terms of films thickness, since with increasing the substrate temperature films became thicker (the thickness is varied from 120 nm to 245 nm with increasing temperature). Thereafter, the transmittance improvement may originates from the film structure.

The optical energy gap for the direct allowed transition between valence bands and conduction bands of ZnS thin films was calculated from equation (2) using $r = 1/2$.

$$(\alpha hv) = A(\alpha h - E_g)^r \quad (2)$$

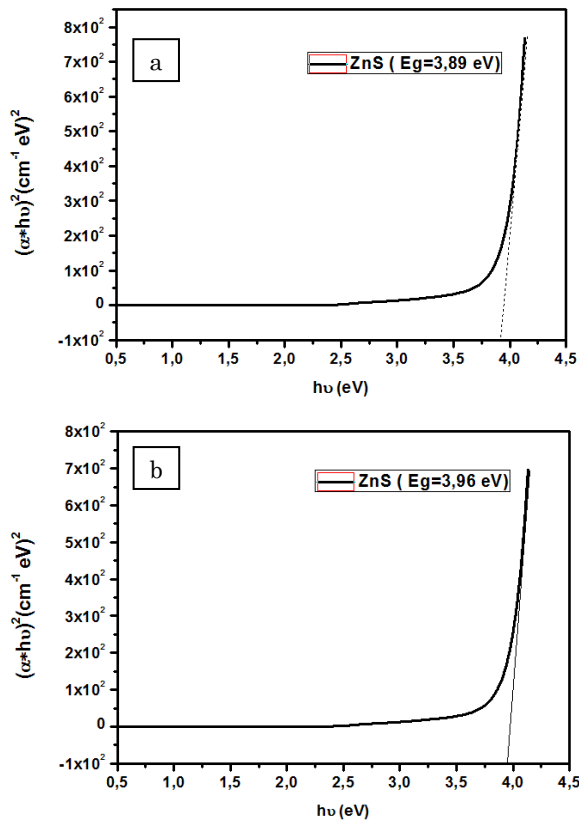


Fig. 7 – The optical energy gap of ZnS thin films prepared: a) at substrate temperature ($T_s = 350\text{ }^\circ\text{C}$), b) at substrate temperature ($T_s = 400\text{ }^\circ\text{C}$)

ZnS is a direct band gap material; several workers reported this type of transition. The energy gaps of the

films of various substrate temperatures have been determined by extrapolating the linear portion of the plots of $(\alpha hv)^2$ against hv (eV) to the energy axis.

The band gap value was determined from the intercept of the straight-line portion of the $(\alpha hv)^2$ against the graph on the hv axis (see Fig. 7).

The band gap energies are calculated to be between 3.89-3.96 eV for the ZnS films with different substrate temperatures. The wide direct band gap makes these films good material for potential applications in optoelectronic devices such as multilayer dielectric filters, and solar cell due to decreases the window absorption losses and that will improves the short circuit current of the cell.

5. CONCLUSION

Chemical spray pyrolysis method was used successfully to synthesize ZnS thin films from a double-source precursor at substrate temperatures of 300, 350, and 400 °C. Studies on morphological, structural and optical properties were performed on the samples using scanning electron microscope (SEM), X-ray diffraction (XRD), Energy Dispersive X-ray analysis (EDAX), Fourier Transform Infrared Spectroscopy (FTIR), and UV-VIS spectrophotometer (UVS).

We noted that film structure composition and optical properties are very sensitive to the deposition temperature. At low deposition temperature films are amorphous. With increasing T_s , the films became polycrystalline with (111) preferential orientation with a stoichiometric ZnS composition. EDAX and FTIR data confirm the formation of ZnS nanoparticles. In our experiment, based on the optical transmission measurements, the band gap energies are calculated to be between 3.89-3.96 eV for the ZnS films with different thicknesses. The optical studies also revealed band gap dependence on substrate temperatures. The wide energy band gap $E_g > 3.50$ and high transmittance make the ZnS film suitable for solar cell and opto-electronic applications.

ACKNOWLEDGMENTS

This work was supported by all members of Laboratory of Electron Microscopy and Materials Sciences University of Science and Technology of Oran and Centre de Recherche en Technologie des Semi-Conducteurs pour l'Energétique 'CRTSE', Algeria. The authors would like to thank Algerian Ministry of Higher Education and Scientific Research and Directorate General for Scientific Research and Technological Development.

REFERENCES

1. S. Yamaga, A. Yoshokawa, H. Kasain, *J. Cryst. Growth* **86**, 252 (1998).
2. I.C. Ndukwe, *Sol. Energ. Mater. Sol. C.* **40**, 123 (1996).
3. T.E. Varitimos, R.W. Tustison, *Thin Solid Films* **151**, 27 (1987).
4. J. Vidal, O. de Melo, O. Vigil, N. Lopez, G. Contreras-Puente, O. Zelaya-Angel, *Thin Solid Films* **419**, 118 (2002).
5. H.L. Kwok, *J. Phys. D: Appl. Phys.* **16**, 2367 (1983).
6. O.M. Hussain, P.S. Reddy, B.S. Naidu, U. Uthanna, P.J. Reddy, *Semicond. Sci. Technol.* **6**, 690 (1991).
7. M.P. Valkonen, S. Lindroos, T. Kanninen, M. Leskela, U. Tapper, E. Kauppinen, *Appl. Surf. Sci.* **120**, 58 (1997).
8. Y.F. Nicolau, J.C. Menard, *J. Crystal Growth* **92**, 128 (1988).
9. G. Xu, S. Ji, C. Miao, G. Liu, C. Ye, *J. Mater. Chem.* **22**, 4890 (2012).
10. H.M. Pathan, C.D. Lokhande, *Bull. Mater. Sci.* **27**, 85 (2004).
11. L.-X. Shaoi, K.-H. Chang, H.-L. Hwang, *Appl. Surf. Sci.* **212**, 213 (2003).
12. H. Lekiket, M.S. Aida, *Mater. Sci. Semicond. Proc.* **16**, 1753 (2013).
13. P. Roy, J.R. Ota, S.K. Srivastava, *Thin Solid Films* **515**, 1912 (2006).
14. T. BenNasr, N. Kamoun, M. Kanzari, R. Bennaceur, *Thin Solid Films* **500**, 4 (2006).
15. F. Göde, C. Gümüş, M. Zor, *J. Cryst. Growth* **299**, 136 (2007).
16. G.L. Agawane, S.W. Shin, A.V. Moholkar, K.V. Gurav, J.H. Yun, J.Y. Lee, J.H. Kim, *J. Alloy. Compd.* **535**, 53 (2012).
17. T. Lwushita, S.Z. Shi, *Thin Solid Films* **520**, 7076 (2012).
18. Z.Q. Li, J.H. Shi, Q.Q. Liu, Z.A. Wang, Z. Sun, S.M. Huang, *Appl. Surf. Sci.* **257**, 676 (2010).
19. K. Ichino, T. Onishi, Y. Kawakami, S. Fujita. *J. Crystal Growth* **138**, 28 (1994).
20. Z.J. Xin, R.J. Peaty, H.N. Rutt, R.W. Eason, *Semicond. Sci. Technol.* **14**, 695 (1999).
21. T.L. Chu, S.S. Chu, J. Britt, C. Feredikes, C.Q. Wu, *J. Appl. Phys.* **70**, 2688 (1991).
22. S. Lindroos, G. Rusu, *J. Optoelectron. Adv. Mater.* **7**, 817 (2005).
23. S.S. Nath, D. Chakdar, G. Gope, *Nanotrends- A journal of nanotechnology and its application* 02, 03 (2007).
24. S.S. Nath, D. Chakdar, G. Gope, D.K. Avasthi, *J. Nanoelectron. Optoelectron.* **3**, 180 (2008).
25. B.D. Hall, D. Zanchet, D. Ugarte, *J. Appl. Crystallography* **33**, 1335 (2000).
26. Ali A. Yousif, Aseel A. Jasib, *Int. J. Innovative Sci., Engin. Technol.* **2** No 3, 886 (2015).